Measurement of the $^{199}Hg^+$ $5d^9 6s^2\,{}^2D_{5/2}$ Electric Quadrupole Moment and a Constraint on the Quadrupole Shift

W. H. Oskay, W. M. Itano, and J. C. Bergquist*

Time and Frequency Division, National Institute of Standards and Technology, 325 Broadway, Boulder, Colorado 80305, USA

(Received 22 November 2004; published 26 April 2005)

The electric-quadrupole moment of the $^{199}Hg^+$ $5d^9 6s^2\,{}^2D_{5/2}$ state is measured to be $\Theta(D, 5/2) = -2.29(8) \times 10^{-40}\ \mathrm{C\,m^2}$. This value was determined by measuring the frequency of the $^{199}Hg^+$ $5d^{10}6s\,{}^2S_{1/2} \rightarrow 5d^9 6s^2\,{}^2D_{5/2}$ optical clock transition for different applied electric-field gradients. An isolated, mechanically stable optical cavity provides a frequency reference for the measurement. We compare the results with theoretical calculations and discuss the implications for the accuracy of an atomic clock based upon this transition. We now expect that the frequency shift caused by the interaction of the quadrupole moment with stray electric-field gradients will not limit the accuracy of the Hg^+ optical clock at the 10^{-18} level.

DOI: 10.1103/PhysRevLett.94.163001 PACS numbers: 32.10.Dk, 06.30.Ft, 32.30.Jc

Atomic frequency standards provide the foundation for a wide range of experiments and precision measurements that not only have produced the most accurately realized determinations of many physical quantities, but that have also produced some of the most stringent tests of our fundamental concepts and theories of nature. For example, recent, highly accurate absolute frequency measurements of several microwave and optical frequency standards have yielded sensitive probes of possible temporal changes of some of the fundamental constants [1–3]. The precision of these measurements was limited by the uncertainties of the systematic frequency shifts of the clock transition in the individual atomic frequency standards. In these and other experiments, greater sensitivity would be possible with atomic frequency standards that obtain inaccuracy below the 1 part in 10^{15} typical of the best, present-day atomic standards—the cesium fountain standards [4], which provide both the definition and realization of the SI second. Optical frequency standards offer the potential of reaching inaccuracies approaching 1 part in 10^{18}. Many of these standards, based on narrow transitions in either ions or neutral atoms, are being pursued worldwide [5].

The inaccuracy of trapped-ion optical frequency standards based upon weakly allowed, electric-quadrupole transitions in Hg^+ [6], Sr^+ [7], and Yb^+ [8] has been dominated by uncertainty in the electric-quadrupole shift that arises from the interaction of the excited state electric-quadrupole moment with stray electric-field gradients. Preliminary reports of a quadrupole shift in Hg^+ [9] and the quadrupole moment of Yb^+ [8] have previously been reported, but have done little to constrain possible error due to the quadrupole shift. A recent measurement of the Sr^+ quadrupole moment [7], made by measuring the shift in the absolute frequency of the clock transition for several applied electric-field gradients, has now demonstrated that inaccuracy below 10^{-15} is possible in that species.

In this Letter we report an experimental measurement of the $^2D_{5/2}$ electric-quadrupole moment of the mercury ion and compare it to theory. We determined its value by measuring the frequency shift of the $5d^{10}6s\,{}^2S_{1/2}(F = 0) \rightarrow 5d^9 6s^2\,{}^2D_{5/2}$ $(F = 2,\ m_F = 0)$ electric-quadrupole transition in a single $^{199}Hg^+$ ion with respect to the resonance of a highly stable optical cavity [10] for various applied electric-field gradients and magnetic-field orientations. A major advantage of this technique is its relative speed and simplicity due to the high signal-to-noise ratio afforded by the spectrally narrow laser and stable cavity. The data reported here were collected in less than five hours of operating time, all with the same ion. By measuring the shift without an applied electric-field gradient, we also place an upper bound on the contribution of the quadrupole shift to the uncertainty of the mercury clock.

The electric-field gradient was applied by adding a bias voltage to the end caps of our spherical rf (Paul) trap, which consists of a ring electrode and two end cap electrodes that are ac grounded and normally held near ground potential. The ring electrode was driven with voltage $V(t) = V_0 \cos(\Omega t) - V_{\mathrm{ec}}$ relative to the end caps, where the rf frequency was $\Omega = 2\pi \times 12.007$ MHz. The electrical potential of the trap has the form of a 3D quadrupole, $\Phi(x, y, z, t) = V(t)(x^2 + y^2 - 2z^2)/d_0^2$, where d_0^2 is a geometric factor with dimensions of area. The ion was laser cooled to a temperature of a few millikelvins and the trap potential was made deep enough to resolve the secular sidebands [11]. To determine d_0, we measured the secular frequency in the radial direction ν_{r} as a function of V_0 and V_{ec}. Fitting the results to the known dependence of ν_{r} on these parameters, we found $d_0^2 = 1.08(1)\ \mathrm{mm^2}$, where the uncertainty is limited by the use of a fitting model that neglects high-order terms [12]. The static component of the quadrupole field is $A_{\mathrm{Q}} \equiv -V_{\mathrm{ec}}/d_0^2 = -V_{\mathrm{ec}}/(1.08(1)\ \mathrm{mm^2})$ along the trap axis.

We oriented the quantization axis (magnetic-field orientation) at an angle β from the symmetry axis of the trap, $\hat{z}$. Following Ref. [13], the quadrupole shift in the energy of

the clock transition is given by

$$h\Delta\nu_Q = \frac{4}{5}A_Q\Theta(D, 5/2)(3\cos^2\beta - 1), \quad (1)$$

where h is the Planck constant, $\Delta\nu_Q$ is the change in the transition frequency due to A_Q, and $\Theta(D, 5/2)$ is the quadrupole moment of the $^2D_{5/2}$ state. For the quantization axis along the trap axis ($\beta = 0°$), $\Delta\nu_Q = 8A_Q\Theta(D, 5/2)/5h$. If instead the quantization axis is perpendicular to the trap axis, the quadrupole shift is opposite in sign with half the magnitude: $\Delta\nu_Q = -4A_Q\Theta(D, 5/2)/5h$. In general, the quadrupole shift averages to zero over measurements with any three orthogonal quantization axes [13].

Frequency-doubled light from a dye laser at 563 nm was used to probe the clock transition. The frequency of the dye laser was locked to a resonance of a highly isolated, high-finesse ($\mathcal{F} \sim 200\,000$) Fabry-Perot cavity. The locked laser has a fractional frequency instability of about $3–4 \times 10^{-16}$ between 1 and 10 s, corresponding to a linewidth of ~640 mHz at 282 nm [10]. Two acousto-optic modulators (AO1, AO2) shift the frequency of the stabilized light away from the cavity resonance onto the atomic resonance. The frequency f_{AO1} of AO1 was swept to compensate for the predictable linear drift ($\lesssim 1$ Hz/s) of the cavity. AO2 gives a shift f_{AO2} to the frequency of the 563 nm beam. Following AO2, the light was frequency doubled and directed onto the mercury ion. The ion was probed with single 40 ms pulses and the measured linewidth at 282 nm was transform limited to a full width at half maximum (FWHM) of 20 Hz. The frequency f_{AO2} was alternately stepped positive or negative by an increment equal to half the FWHM so as to probe the clock transition on both sides of the resonance. A digital servo system then steers f_{AO1} to match the cavity-stabilized laser frequency to the center of the atomic resonance.

For the measurements of the quadrupole moment, we locked the laser to the atomic resonance and drove V_{ec} with a nearly square modulation waveform with a period of 120 s. The waveform consisted of 59 s segments alternately at $V_{ec} = 0$ V and $V_{ec} = V_A$, separated by 1 s ramps. The same voltage was applied to both end caps, to within 1%, for each value of V_A.

For changes in the clock transition frequency that are small compared to the linewidth, the servo system steers the laser frequency with a time constant near 15 s. To maintain lock and to maximize the signal-to-noise ratio, we implemented a feed-forward system to introduce an estimated step change ν_{est} into the servo system during the 1 s changes in V_{ec}. With an appropriate choice of ν_{est}, the servo stays near equilibrium and follows large changes, independent of the transform-limited linewidth.

We collected data by counting the frequency $2|f_{AO1}|$ with a commercial frequency counter with a gate time of 1 s. A change in $2|f_{AO1}|$ corresponds to twice the change in the frequency at 563 nm and therefore gives the frequency change at 282 nm. Data were collected at four values of V_A for two different orientations of the magnetic field $\mathbf{B}$, $\mathbf{B} \parallel \hat{z}$ and $\mathbf{B} \perp \hat{z}$. Each run was between 30 and 38 min long. The field magnitudes were $|\mathbf{B}| = 1.99(6) \times 10^{-5}$ T, as determined by spectroscopy of the $^2S_{1/2}(F = 0) \rightarrow {}^2D_{5/2}$ ($F = 2$, $m_F = \pm 1$) Zeeman-sensitive lines. Ambiguities in the orientation of $\mathbf{B}$, the ion trap, and the quadrupole field inside the trap lead to an uncertainty in β of $\pm 5°$. Since we are measuring $\Delta\nu_Q$ at local extrema, errors in β can only reduce the shift.

The data analysis procedure (Fig. 1) relies upon the short-term stability of the reference cavity. The raw data from the counter are dominated by the linear drift of the cavity. After subtracting a linear fit, the signal shows both the modulation and the residual drift of the cavity. These data were averaged over a 120 s window to leave only the slowly varying, unmodeled drift. This residual drift was subtracted from the data to yield a nearly square wave signal at the modulation period. Simulations confirm that this procedure does not bias the results of the analysis.

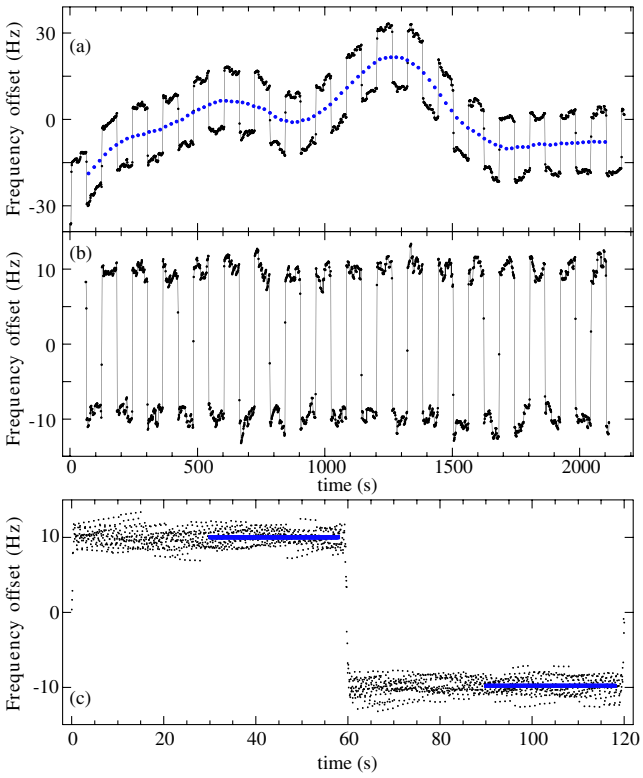

FIG. 1 (color online). Method of data analysis, illustrated with data for $A_Q = 36$ V/mm^2 and $\mathbf{B} \parallel \hat{z}$. The raw data after subtracting the linear drift (a) (solid line) show the 120 s modulation and small unmodeled drift. Averaging over the modulation period leaves only the slowly varying drift (dotted line). Subtracting this drift, we have a signal (b) that contains only the modulation. Plotting these data in a single effective modulation period (c), we measure the amplitude by taking the mean value (solid line) in the range 30 to 58 s after each edge.

Finally, the data were compiled by replotting modulo 120 s. Because the servo may track in towards some final value, data from the first 30 s after each change in V_{ec} were rejected. A 2 s segment of time before each change was also rejected to ensure that the analysis was not influenced by the subsequent change. The amplitude of the signal was determined from the mean value of the data in each remaining segment.

The estimated step frequency ν_{est} was approximately (0.5 Hz/V)V_A for the data points with $\mathbf{B} \parallel \hat{z}$. Two additional data runs were taken for the case $A_Q = 36$ V/mm^2 and $\mathbf{B} \parallel \hat{z}$, where the value of ν_{est} was changed by $\pm 20\%$ from the initial estimate. The compiled data for these runs showed significant tracking in of the frequency. The amplitudes calculated for these runs were displaced by $\pm 5\%$ respectively from their average. For cases with an appropriate choice of ν_{est} (such as that in Fig. 1), no tracking in was visible. Uncertainty due to residual servo error was estimated by taking the standard deviation of the shift measured during the second, third, and fourth 15 s intervals of the modulation period, rather than the usual 28 s interval. This method correctly estimated the $\pm 5\%$ servo errors for the cases where ν_{est} was deliberately offset by $\pm 20\%$. The combined servo error uncertainty and statistical uncertainty of the amplitude at each data point was in the range 0.15 to 0.47 Hz.

The results of the measurements for each $\mathbf{B}$ field orientation at each value of V_A are shown in Fig. 2. Weighted linear fits to the two data sets yielded slopes $-0.550(5)$ Hz/(V/mm^2) for $\mathbf{B} \parallel \hat{z}$, and $+0.261(17)$ Hz/(V/mm^2) for $\mathbf{B} \perp \hat{z}$. The average of the slopes weighted by their variance is $-0.549(6)$ Hz/(V/mm^2) for $\beta = 0°$.

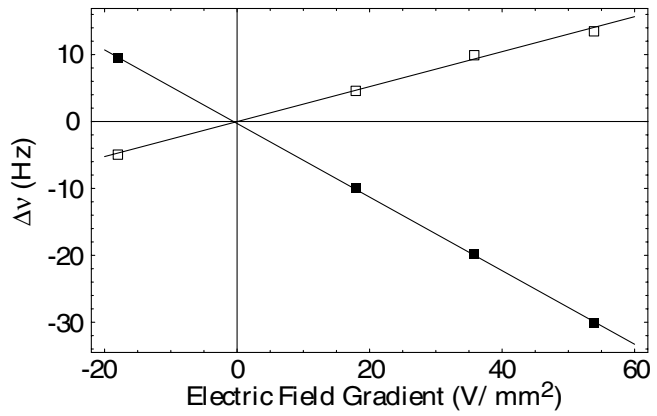

FIG. 2. Quadrupole shift as a function of the electric-field gradient applied to the trap. Data are shown with $\mathbf{B} \parallel \hat{z}$ (filled boxes) and with $\mathbf{B} \perp \hat{z}$ (open boxes). The two curve fits shown are linear with slopes -0.550 Hz/(V/mm^2) and $+0.261$ Hz/(V/mm^2) respectively. Error bars representing the combined servo error uncertainty and statistical uncertainty would be smaller than the symbol at each data point.

At high values of the end cap voltage there was small but detectable excess micromotion [14] for which we did not fully compensate. Excess micromotion can lead to an ac Stark shift and second-order Doppler shift that (in this case) depend upon V_{ec}. While shifts of this type can potentially be large, we are able to constrain them because they both must be independent of $\mathbf{B}$. The fits for both orientations of $\mathbf{B}$ had zero-offset frequencies below 0.3 Hz and a difference in slope that agreed with the expected factor of -2 to within the slope uncertainty. Using that uncertainty, we estimate that the error caused by micromotion in determining the slope is bounded by $\pm 3\%$. There is also uncertainty in the slope due to uncertainty in the calibrations of d_0 ($\pm$ 1%) and β ($\pm$ 1.1%). We made a correction of $+0.5\%$ in the absolute value of the slope to compensate for bias due to the uncertainty in determining β to arrive at a final slope of $-0.552(19)$ Hz/(V/mm^2). From Eq. (1), the quadrupole moment was thus measured to be $\Theta(D, 5/2) = -(5h/8) \times 0.552(19)$ Hz mm^2/V $= -2.29(8) \times 10^{-40}$C m^2 $= -0.510(18) e a_0^2$, where a_0 is the Bohr radius.

A single-configuration Hartree-Fock calculation with the Cowan code [15] predicts $\Theta(D, 5/2) = -0.664 e a_0^2$ [13]. The results of a multiconfiguration Dirac-Hartree-Fock (MCDHF) [16,17] calculation of $\Theta(D, 5/2)$ are shown in Table I. Three successively larger sets of virtual orbitals were generated by minimizing the sum of the energies of the lowest $^2D_{5/2}$ and $^2D_{3/2}$ states, weighted by $(2J + 1)$, keeping the previously determined orbitals fixed. The orbitals added to the reference $5d^9 6s^2\, ^2D_{5/2,3/2}$ configurations are listed for Stages 2, 3, and 4. Sets of configuration state functions were generated by allowing single and double excitations to the virtual orbitals from the $6s$ valence and the $\{5s, 5p, 5d\}$ core shells, with at most one excitation from the core. At Stage 5, some core-core correlation was included by adding configuration state functions with up to two excitations from the $\{5s, 5p, 5d\}$ core and up to three excitations from the $\{5d, 6s\}$ set of shells to the virtual $\{7s, 6p, 6d, 5f\}$ orbitals. Stage 5 was a configuration-interaction calculation in which the Hamiltonian matrix was diagonalized, using the orbitals

TABLE I. Sequence of calculations with an expanding set of virtual orbitals and core excitations. For each stage of the calculation, the quadrupole moment $\Theta(D, 5/2)/e a_0^2$ and the hyperfine constant A are given.

Stage	Description	$\Theta/e a_0^2$	A (MHz)
1	Reference	-0.6887	991.1
2	$+\{7s, 6p, 6d, 5f, 5g, 6h\}$	-0.5299	1087.1
3	$+\{8s, 7p, 7d, 6f, 6g\}$	-0.5460	940.2
4	$+\{9s, 8p, 8d\}$	-0.5421	910.9
5	$+\{5s, 5p, 5d\}$ core-core	-0.5463	926.1
6	$+\{3d, 4s, 4p, 4d, 4f\}$ core-valence	-0.5440	963.5

determined at Stage 4. In Stage 6, additional core-valence correlation was included by adding single excitations from the $\{3d, 4s, 4p, 4d, 4f\}$ shells, with or without a single $6s$ excitation, to the full Stage 4 set of virtual orbitals, in a configuration-interaction calculation. The final result for $\Theta(D, 5/2)$ is $-0.5440ea_0^2$, about 7% larger in magnitude than the experimental value. The hyperfine constant A also was evaluated at each stage. The final result for A was 963.5 MHz, about 2.3% smaller than the experimental value of A of 986.19(4) MHz [13]. The discrepancies are probably due to neglected core-valence and core-core correlation terms. No other calculations of $\Theta(D, 5/2)$ have been reported. Brage *et al.* [18] obtained a value for A of the $5d^9 6s^2\, ^2D_{5/2}$ state of Hg^+ of 1315 MHz, using the MCDHF method with a less extensive set of relativistic configuration state functions.

We have also calculated the quadrupole moments of the $5d\, ^2D_{5/2}$ state of Sr^+ and of the $4d\, ^2D_{3/2}$ state of Yb^+, for which recent measurements are available [7,8]. The MCDHF results are $\Theta(D, 5/2) = 2.99ea_0^2$ for Sr^+ and $\Theta(D, 3/2) = 2.04ea_0^2$ for Yb^+. The experimental values are $2.6(3)ea_0^2$ for Sr^+ [7] and $3.9 \pm 1.9ea_0^2$ for Yb^+ [8].

The error budget for the mercury-ion clock has thus far been dominated by a conservatively chosen ± 10 Hz [19] on the quadrupole shift due to stray electric-field gradients. The field gradient and orientation are unknown, so knowing the quadrupole moment alone does not constrain the shift. Likewise, the results of an earlier measurement in a linear ion trap [9] do not constrain the shift in the spherical trap. After our measurements of the quadrupole moment, we looked for a frequency shift of the clock transition but without applying a significant end cap voltage (voltages of ± 7 mV on the two end caps were applied to compensate for stray patch charges). We switched the **B** field orientation between two axes of an orthogonal coordinate system with a 120 s period, and repeated this procedure with a different pair of axes. The maximum quadrupole shift along these axes was measured to be 0.33 ± 0.34 Hz. The error in the clock frequency due to the quadrupole shift is thus constrained below 1 Hz, when the quantization axis is one of these axes. With the present inaccuracy of magnetic-field alignment, averaging over measurements along the three axes should suppress the shift by a factor of 200, constraining the residual quadrupole shift to below ± 10 mHz, a fractional frequency error of less than 10^{-17}. With improved field alignment, the shift is not expected to limit the accuracy of the clock at the 10^{-18} level. We are also considering an alternative approach [20] to nulling the quadrupole shift, where the shift is averaged over magnetic sublevels rather than field orientation.

Short of a full evaluation versus a second optical frequency standard, it is difficult to further constrain the systematic shifts of the mercury clock. Shifts due to excess micromotion are now expected to be a dominant source of error. At present, we conservatively estimate that the total uncertainty will be less than or equal to ± 1 Hz for future measurements of the clock frequency when nulling out the quadrupole shift.

We thank Till Rosenband and David Wineland for their contributions to this work and Chris Oates and John Hall for careful reading of the manuscript. This work was partially supported by the Office of Naval Research.

*Electronic address: berky@boulder.nist.gov

[1] H. Marion *et al.*, Phys. Rev. Lett. **90**, 150801 (2003).
[2] S. Bize *et al.*, Phys. Rev. Lett. **90**, 150802 (2003).
[3] E. Peik, B. Lipphardt, H. Schnatz, T. Schneider, Chr. Tamm, and S. G. Karshenboim, Phys. Rev. Lett. **93**, 170801 (2004).
[4] *Proceedings of the 6th Symposium on Frequency Standards and Metrology*, edited by P. Gill (World Scientific, Singapore, 2002).
[5] *Frequency Measurement and Control: Advanced Techniques and Future Trends*, edited by A. N. Luiten (Springer Verlag, Berlin, 2001).
[6] S. Diddams *et al.*, Science **293**, 825 (2001).
[7] G. P. Barwood, H. S. Margolis, G. Huang, P. Gill, and H. A. Klein, Phys. Rev. Lett. **93**, 133001 (2004).
[8] Chr. Tamm, T. Schneider, and E. Peik, in *Laser Spectroscopy Proceedings of the XVI International Conference*, edited by P. Hannaford, A. Sidorov, H. Bachor, and K. Baldwin (World Scientific, Singapore, 2004), p. 40.
[9] R. J. Rafac, B. C. Young, J. A. Beall, W. M. Itano, D. J. Wineland, and J. C. Bergquist, Phys. Rev. Lett. **85**, 2462 (2000).
[10] B. C. Young, F. C Cruz, W. M. Itano, and J. C. Bergquist, Phys. Rev. Lett. **82**, 3799 (1999).
[11] J. C. Bergquist, W. M. Itano, and D. J. Wineland, Phys. Rev. A **36**, R428 (1987).
[12] Pradip K. Ghosh, *Ion Traps*, (Oxford University Press, New York 1995).
[13] Wayne M. Itano, J. Res. Natl. Inst. Stand. Technol. **105**, 829 (2000).
[14] D. J. Berkeland, J. D. Miller, J. C. Bergquist, W. M. Itano, and D. J. Wineland, J. Appl. Phys. **83**, 5025 (1998).
[15] R. D. Cowan, *The Theory of Atomic Structure and Spectra* (University of California Press, Berkeley CA, 1981).
[16] F. A. Parpia, C. Froese Fischer, and I. P. Grant, Comput. Phys. Commun. **94**, 249 (1996).
[17] P. Jönsson, F. A. Parpia, and C. Froese Fischer, Comput. Phys. Commun. **96**, 301 (1996).
[18] T. Brage, C. Proffitt, and D. S. Leckrone, Astrophys. J. **513**, 524 (1999).
[19] T. Udem *et al.*, Phys. Rev. Lett. **86**, 4996 (2001).
[20] P. Dubé, L. Marmet, A. A. Madej, and J. E. Bernard, Proceedings of the 2004 Conference on Precision Electromagnetic Measurements, London, 27 June to 2 July 2004.